sciendo

Int. J. of Applied Mechanics and Engineering, 2021, vol.26, No.2, pp.11-30
DOI: 10.2478/ijame-2021-0017

THERMAL PERFORMANCE ENHANCEMENT OF THE MIXED CONVECTION BETWEEN TWO PARALLEL PLATES BY USING TRIANGULAR RIBS

K.A. JEHHEF*, F.A. BADAWY and A.A. HUSSEIN
Middle Technical University, Institute of Technology
Department of Mechanical Power, Baghdad, IRAQ
E-mail: kadhumaudaa@mtu.edu.iq

This paper aims to investigate the mixed convection between two parallel plates of a vertical channel, in the presence of a triangular rib. The non-stationary Navier-Stokes equations were solved numerically in a two-dimensional formulation for the low Reynolds number for the laminar air flow regime. Six triangular ribs heat-generating elements were located equidistantly on the heated wall. The ratio of the ribs to the channel width is varied $(h/H = 0.1,\ 0.2,\ 0.3$ and $0.4)$ to study the effect of ribs height effects, the ratio of the channel width to the ribs height is fixed constant at $(H/w = 2)$ and the ratio of the channel height to the ribs pitch is fixed at (*W/p=10*). The influence of the Reynolds number that ranged from *68* to *340* and the Grashof number that ranged from 6.6×10^3 to 2.6×10^4 as well as the Richardson number chosen $(1.4,\ 0.7,\ 0.4$ and $0.2)$ is studied. The numerical results are summarized and presented as the profile of the Nusselt number, the coefficient of friction, and the thermal enhancement factor. The contribution of forced and free convection to the total heat transfer is analyzed. Similar and distinctive features of the behavior of the local and averaged heat transfer with the variation of thermal gas dynamic and geometric parameters are investigated in this paper. The results showed that the Nusselt number and friction factor increased by using the attached triangular ribs, especially when using the downstream ribs. Also, the results revealed that the Nusselt number increased by increasing the ratio of the ribs to the channel width.

Key words: numerical study, mixed convection, vertical channel, triangular rib.

1. Introduction

The study of mixed convection between two parallel plates in the occurrence of alternating thermal generating elements on the wall is important for in building thermo-physics and printed circuit boards form. As a rule, narrow channels with parallel plates, on which electronic chips are located with sizes comparable to the distance between the parallel plates [1, 2]. In this case, for simplicity requirements, the flow can be considered two-dimensional, and it can be both natural or mixed convection. However, it is limited in its capabilities during intense heat dissipation; therefore, additional forced supply of the heat carrier can lead to a significant intensification of heat transfer [3].

Interest in the problem of mixed convection arose in the second half of the last century, and many numerical and experimental studies were mode. Madhusudhana and Narasimham [4] studied thermal problems of the cooling microelectronics. Extensive experimental and numerical investigations of the influence of a large number of factors on local and integral heat transfer for similar systems of heat-generating elements were made by Sawant and Gururaja [5]. The problems in conjugate formulation take into account the influence of radiant heat transfer and conduction of the bounding walls [6]. Much consideration is given to theoretical and experimental resolve of the optimal heat transfer regimes when varying the thermal and aerodynamic regimes and geometric parameters [7]. However, most of the works were done for the regime of natural convection, or for a forced-convective flow. For mixed convection, as the most common heat transfer case in practice, the number of studies is very limited. Of particular importance is the study of aerodynamics and heat transfer at

* To whom correspondence should be addressed

the flow stabilization section, where the heat transfer coefficients vary greatly depending on the location of the module. Mallikarjun and Vaidya [8] studied the impact of thermal radiation and viscous dissipation on the convective heat transfer flow in a vertical channel. They reflected the Boussinesq and Rosesel approximations in the modeling of mixed convection by conduction and radiation relation with boundary conditions. Their results were presented graphically for various guiding parameters such as the Brinkman number and different wall temperatures. They found that viscous dissipation advanced the flow reversal in the case of a downward flow. Basant and Michael [9] studied the fully developed mixed convection heat transfer of a viscous fluid flow between two vertical channels. The Reynolds model was used to apprehend the change in viscosity with temperatures. They noted that an increase in the parameter of variation of viscosity increases at the same time the speed of the fluid in addition to the skin friction on the heated wall. In the PV cells, not all the absorbed solar energy will have changed into electricity energy but some of it will be converted into heat energy, which should be dispelled by some cooling techniques [10]. The cooling is obtained by inserting triangular ribs in the duct of the solar cell. In order to present a parametric analysis of the influence of the number and size of the ribs, the wind speed, the solar irradiance and the speed of the input fluid on the average temperature of the solar cells and the air as well as electrical and thermal yields of the module. They reported that the triangular ribbed channels are a very effective cooling technique due to the fact that they significantly reduce the average temperature of the PV cell, especially when increasing the number of ribs.

The objective of the present study is to investigate the effect of using up and downward types of triangular ribs along the heated wall of two parallel plates on the hydrodynamic and thermal performance of low Reynolds number mixed convection heat transfer. The present numerical investigation uses many flow and thermal parameters that affect the convection flow between the plates.

2. Problem formulation

In the present study, a numerical research of mixed convection of air flow between two parallel plates is carried out. On the heated wall there are six triangular ribs located equidistantly as shown in Fig.1. The choice of such a number of ribs was determined by the fact that in the studied range of parameters the flow acquires a periodic character already at the fourth or sixth rib. The main reason of this investigation is to determine the boundaries of the operating parameters at which a transition of the predominant influence of mixed convection is observed, as well as to identify the common and distinctive features of heat transfer mechanisms when changing the geometry of the ribs. The shape of the ribs was triangular, the ratio of the rib to the channel width is varied by $(w/W = 0.1,\ 0.2,\ 0.3$ and $0.4)$, the channel height to ribs width is fixed at $(H/w = 2)$ and the channel height to the ribs pitch is fixed at $(L/p = 10)$. The distance between the ribs was equal to their pitch (p).

The walls of the channel, including the places where the ribs were located are assumed to be thermally insulated, and the entire surface of each rib, except for the place of its conjugation with the channel wall is subjected to a constant heat flux q''. At the channel inlet (from below), u_o the forced air flow rate with constant velocity and T_o is the temperature.

The mathematical model of the presented problem was solved by using the two-dimensional Navier-Stokes equations and laminar heat transfer. The influence of gravity is also considered in the Boussinesq approximation. The processing medium is air with the Prandtl number $\mathrm{Pr} = 0.72$. In addition to the effect of the geometric parameters that include the ratio of the rib to channel width, the channel height to ribs width is fixed at (H/w) and the channel height to the ribs pitch is fixed at (L/p), the problem is determined by three dimensionless quantities, i.e. the Reynolds number, Richardson number and Grashof number. In this study, the low Reynolds number varied in the range as follow [11]:

$$\mathrm{Re} = \frac{u_o H}{v} = 68 \text{ to } 340 \tag{2.1}$$

and Grashof numbers are given by:

$$\mathrm{Gr} = \frac{g\beta q'' H^4}{k\nu^2} = 10^3 \quad \text{to} \quad 10^4 . \tag{2.2}$$

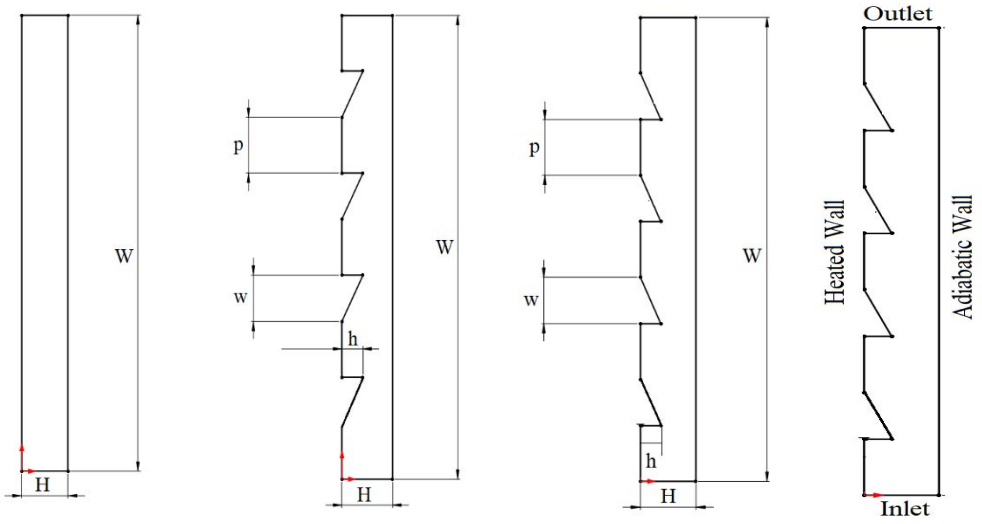

Fig.1. Schematic of the problem geometry, a) smooth channel, b) upward triangular ribs, c) downward triangular ribs and d) boundary conditions.

Thus the Richardson number is formulated as:

$$\mathrm{Ri} = \frac{\mathrm{Gr}}{\mathrm{Re}^2} = 0.2 \quad \text{to} \quad 1.4 . \tag{2.3}$$

The air flow under such conditions was described by the Navier-Stokes equations for a Newtonian fluid in the Boussinesq approximation. These equations can be represented in dimensionless equations in the form of continuity equation [12]:

$$\frac{\partial U}{\partial X} + \frac{\partial V}{\partial Y} = 0 , \tag{2.4}$$

and momentum equations [13]:

$$\frac{\partial U}{\partial \tau} + U\frac{\partial U}{\partial X} + V\frac{\partial U}{\partial Y} = -\frac{\partial P}{\partial X} + \left(\frac{\mathrm{Pr}}{\mathrm{Ra}}\right)^{1/2}\left(\frac{\partial^2 U}{\partial X^2} + \frac{\partial^2 U}{\partial Y^2}\right) , \tag{2.5}$$

$$\frac{\partial V}{\partial \tau} + U\frac{\partial V}{\partial X} + V\frac{\partial V}{\partial Y} = -\frac{\partial P}{\partial Y} + \left(\frac{\mathrm{Pr}}{\mathrm{Ra}}\right)^{\frac{1}{2}}\left(\frac{\partial^2 V}{\partial X^2} + \frac{\partial^2 V}{\partial Y^2}\right) + \theta, \tag{2.6}$$

and energy equation:

$$\frac{\partial \theta}{\partial \tau} + U\frac{\partial \theta}{\partial X} + V\frac{\partial \theta}{\partial Y} = (\mathrm{Ra}\,\mathrm{Pr})^{-\frac{1}{2}}\left(\frac{\partial^2 \theta}{\partial X^2} + \frac{\partial^2 \theta}{\partial Y^2}\right) + \theta . \tag{2.7}$$

The skin friction factor, C_f is given by:

$$C_f = 2\tau_w / \rho \bar{U}^2 . \tag{2.8}$$

The friction factor, f is computed as:

$$f = 2\left(\frac{\Delta P}{L}\right) D_h / \rho \bar{U}^2 . \tag{2.9}$$

The local Nusselt number Nu_x, is:

$$\mathrm{Nu}_x = h_x D_h / k_f . \tag{2.10}$$

The average Nusselt number Nu, can be gained by:

$$\mathrm{Nu} = \frac{1}{H}\int_0^L \mathrm{Nu}_x \, dx . \tag{2.11}$$

The Thermal Enhancement Factor, TEF is given by:

$$\mathrm{TEF} = \left(\mathrm{Nu}/\mathrm{Nu}_o\right) / \left(f / f_o\right)^{1/3} . \tag{2.12}$$

The boundary conditions of air fluid flow between two parallel plates are described as follow:

At the inlet, $x = 0$:

$$u = u_{in} , \tag{2.13}$$

$$v = 0 , \tag{2.14}$$

$$T = T_{in} . \tag{2.15}$$

At the outlet, $x = L$:

$$P = P_{atm} , \tag{2.16}$$

$$\frac{\partial \theta}{\partial x} = 0, \quad \frac{\partial U}{\partial x} = 0, \quad \frac{\partial V}{\partial x} = 0 . \tag{2.17}$$

At the walls, $x = H/2$ and $x = -H/2$:

$$U = v = 0 , \tag{2.18}$$

$$q = q" . \tag{2.19}$$

3. Numerical solution

In the numerical solution Eqs (2.9)-(2.11) were discretized according to a semi-implicit scheme in which convective terms were approximated by the second-order Adams-Bashfort method, and diffusion ones by the Crank-Nicholson scheme. To approximate the spatial derivatives, the central differences of the second order of accuracy were used. For the numerical solution of the system of Navier-Stokes equations, the control volume method of the second order of accuracy was used. To satisfy the continuity equation with the velocity field and determine the pressure field, the SIMPLEC algorithm was used. The number of cells of the structured computational grid was determined in preliminary test calculations (at the maximum values of the Re, Ri and Gr parameters) so that its further refinement did not lead to any significant changes, both in the integral and local flow characteristics. Note that the software package ANSYS-Fluent v.16.2 has been thoroughly tested and successfully used to solve problems of forced and free-convection flows. At the preliminary stage, an analysis was made of the influence of the number of grid nodes on the accuracy of the resulting solution. As a result, it was found that a sufficient degree of accuracy is achieved using (*402201* nodes) for the smooth vertical channel model, (*613495* nodes) for the upward model and (*714261* nodes) for the downward model grid for the domain between two parallel plates as shown in Fig.2. With a further increase in the number of nodes, the change in the distribution of heat fluxes on the wall, vorticity, velocity components, and other parameters did not exceed *0.1%.* The value of the time step was limited by the stability conditions of the numerical scheme at (*0.01* sec) to obtain the stationary solutions, it was selected in such a way as to obtain the numerical solution with minimal computational resources. When considering non-stationary processes, the time step value, as in the case of spatial discretization, was determined so that the solution did not depend on it.

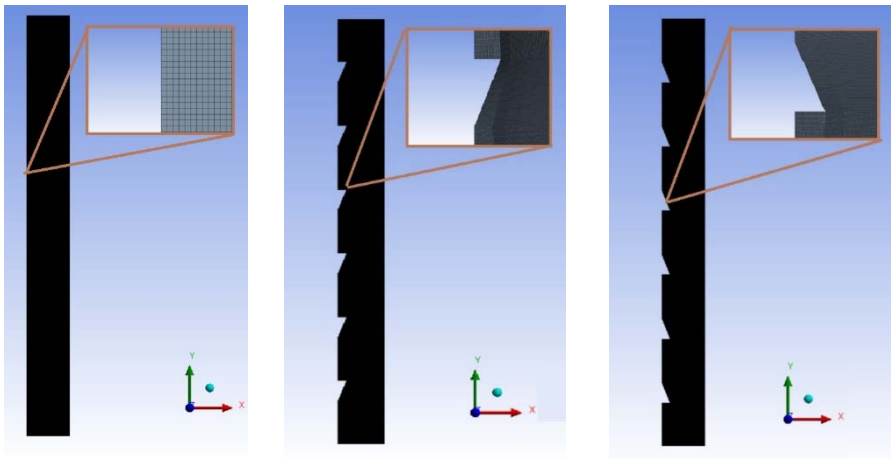

a) Smooth (*402201* nodes) b) Upward (*613495* nodes) c) Downward (*714261* nodes)

Fig.2. Computational domain of the problem smooth (left), upward (center) and downward (right) triangular rib geometry.

4. Results and discussion

The study of heat transfer characteristics for a system of discrete triangular heated ribs is of interest, since such heating systems are often used within engineering applications such as electronic equipment. In this study, the numerical computation was used as the foundation for a comparative examination of heat transfer. In the study the more complex two-dimensional two parallel plates, when separated air flows can play an important role. Moreover, in the calculations the geometry of the problem is fixed except the height of the triangular ribs, and only the Reynolds, Richardson and Grashof numbers changed. The development of the longitudinal pressure, velocity and temperatures contours between the two parallel plates at the same Reynolds number $\mathrm{Re} = 340$ and Grashof numbers $\mathrm{Ri} = 0.2$ and $\mathrm{Gr} = 10^4$ is shown in Figs 3-5, respectively.

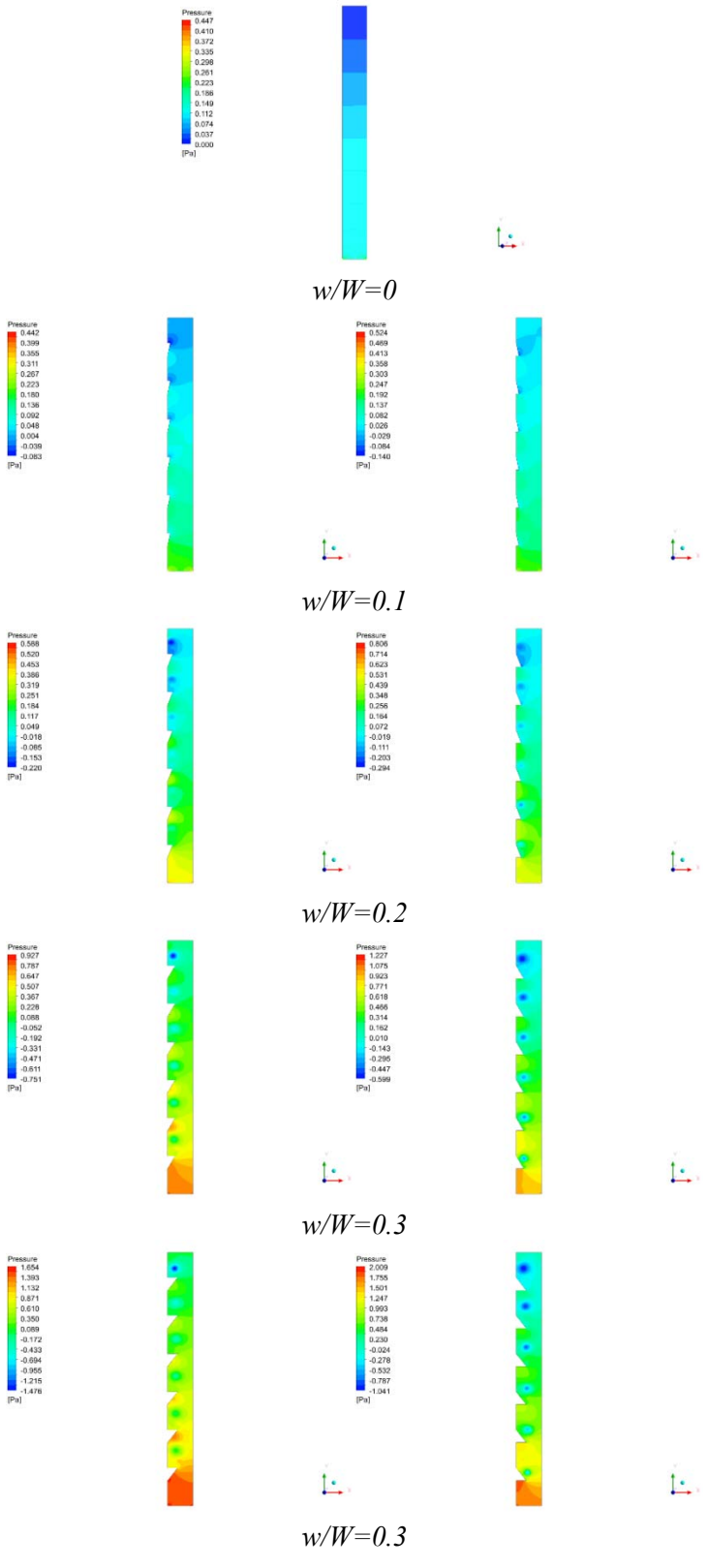

Fig.3. Pressure countors of two parallel plates with triangular ribs upstream (left) and downstream (right) of air flow for various ribs height ratio at $\mathrm{Re} = 340$, $\mathrm{Gr} = 2.6 \times 10^4$ and $\mathrm{Ri} = 0.2$.

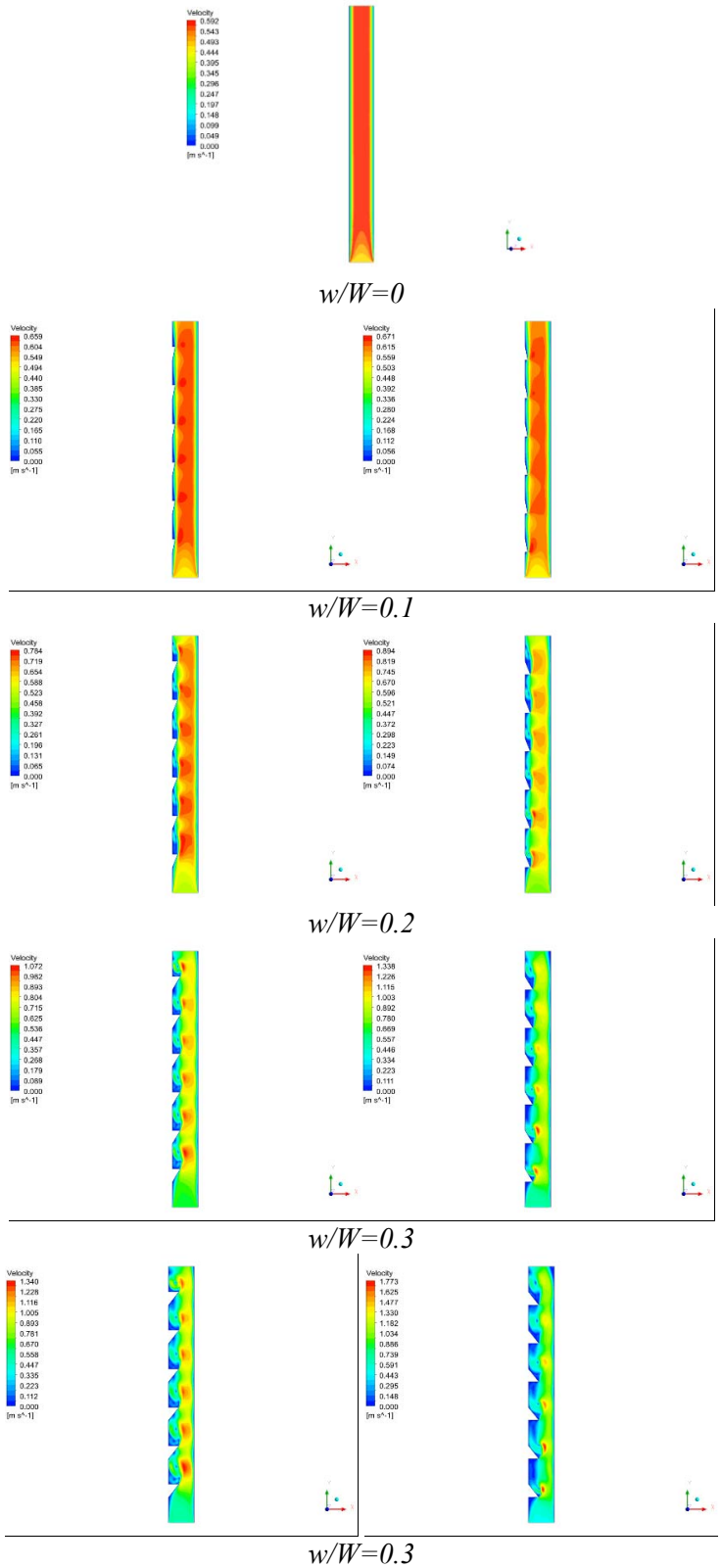

Fig.4. Velocity countors of two parallel plates with triangular ribs upstream (left) and downstream (right) of air flow for various ribs to height ratio at $\mathrm{Re} = 340$, $\mathrm{Gr} = 2.6 \times 10^4$ and $\mathrm{Ri} = 0.2$.

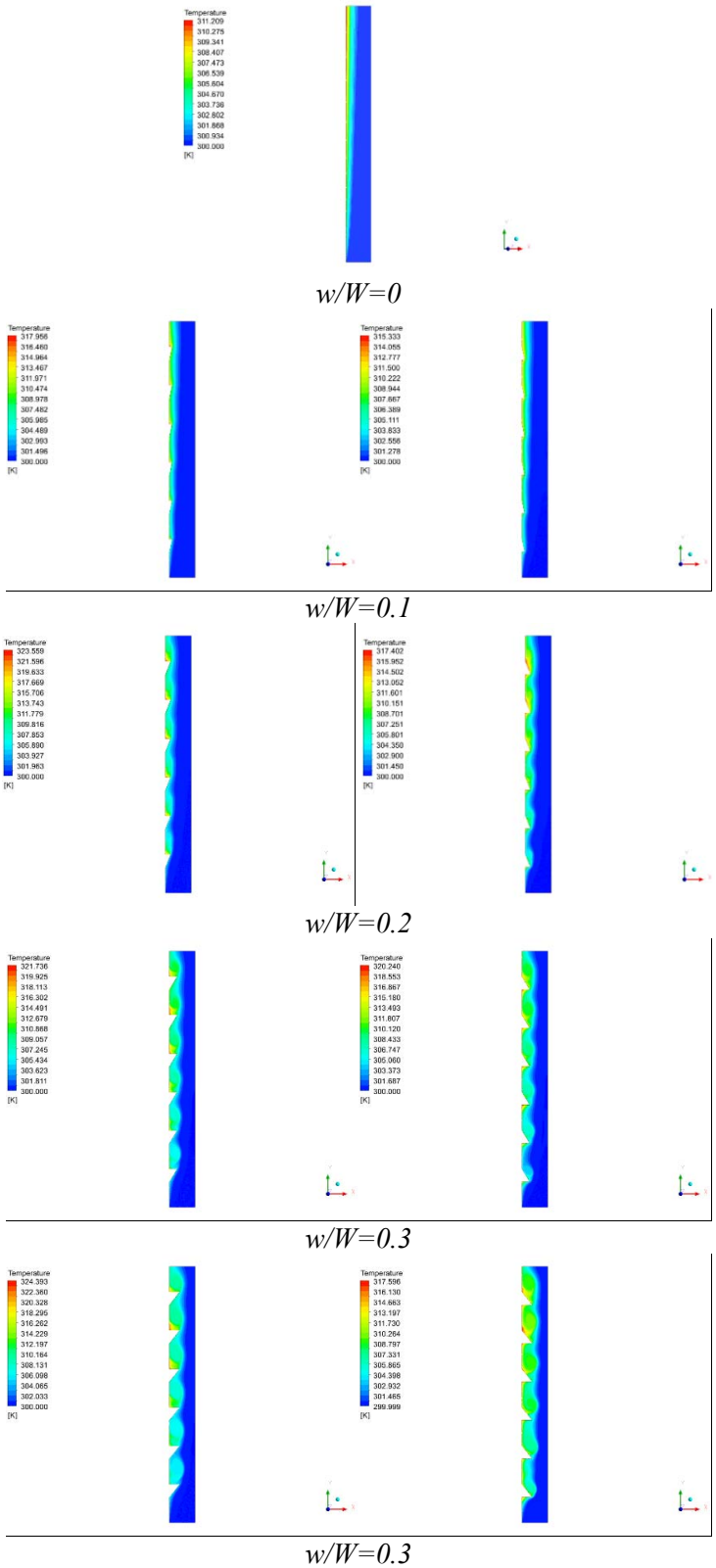

Fig.5. Temperature countors of two parallel plates with triangular ribs upstream (left) and downstream (right) of air flow for various ribs to height ratio at $\mathrm{Re} = 340$, $\mathrm{Gr} = 2.6 \times 10^4$ and $\mathrm{Ri} = 0.2$.

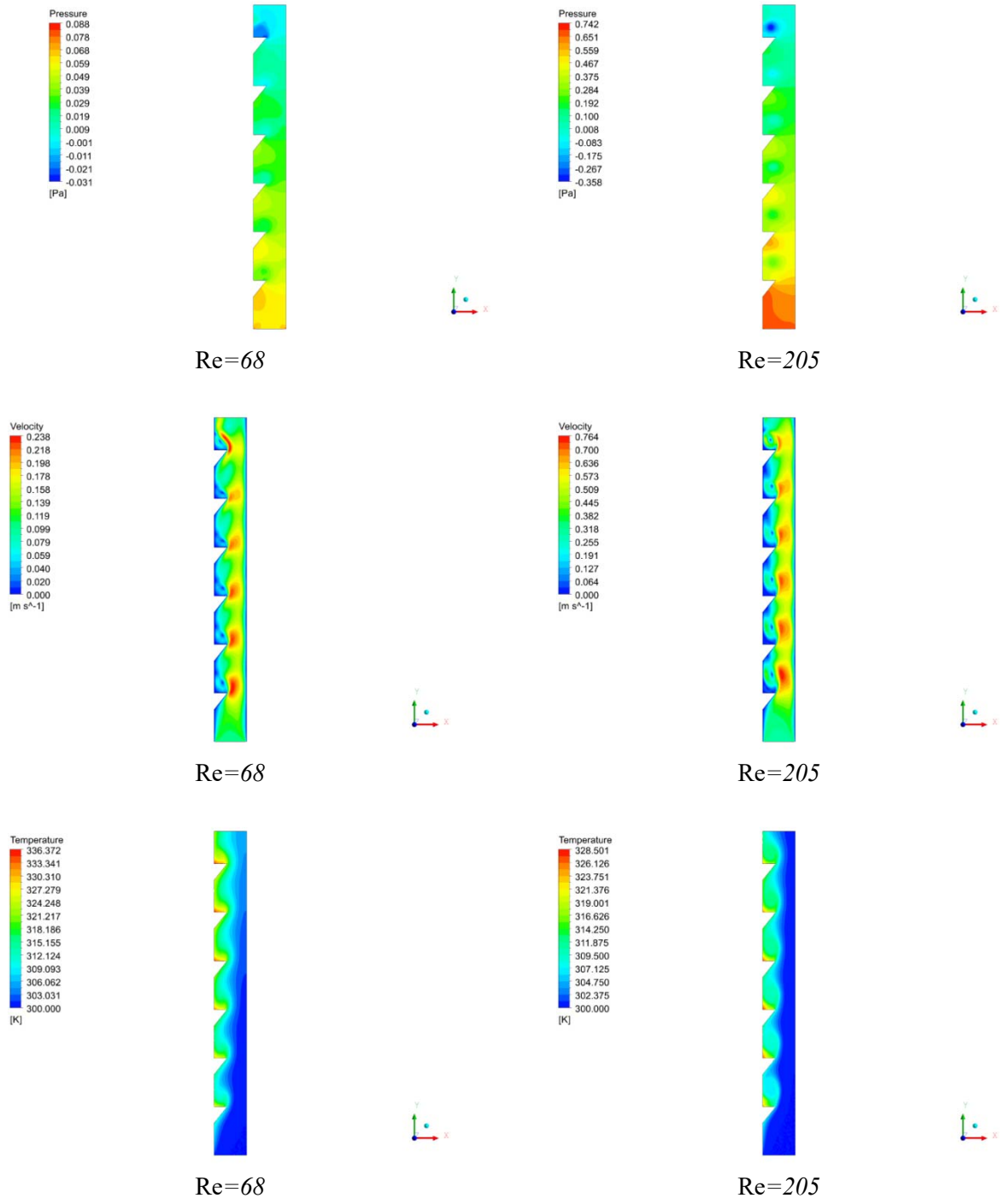

Fig.6. Pressure, velocity and temperature countors of two parallel plates with triangular ribs upstream of air flow for ribs to height ratio of $w/W = 0.4$, $\mathrm{Gr} = 2.6 \times 10^4$ and $\mathrm{Ri} = 0.2$.

Here, each of the contour represents a distribution in the cross section in the entrance and in the middle of each of the parallel plates. As can be seen, the flow stabilizes rather quickly and already towards the first rib in the thermal boundary layer the flow is stratified and takes the form of a classical laminar flow. The pressure drop when using a ribbed heated wall instead of a smooth wall also increases when increasing the height ribs ratio in a limited channel as shown in Fig.3. When using triangular ribs along the heated plate in

the two cases of upward and downward ribs, the figures showed that the flow velocity is restructured along the ribbed wall so that the air flow rate remains the same in height. The results showed that the maximum velocity increased when using upward triangular ribs but it increased more significantly when using downward ribs due to increasing the momentum of the air flow. But in the two cases the velocity increased with increasing the ribs height shown in Fig.4.

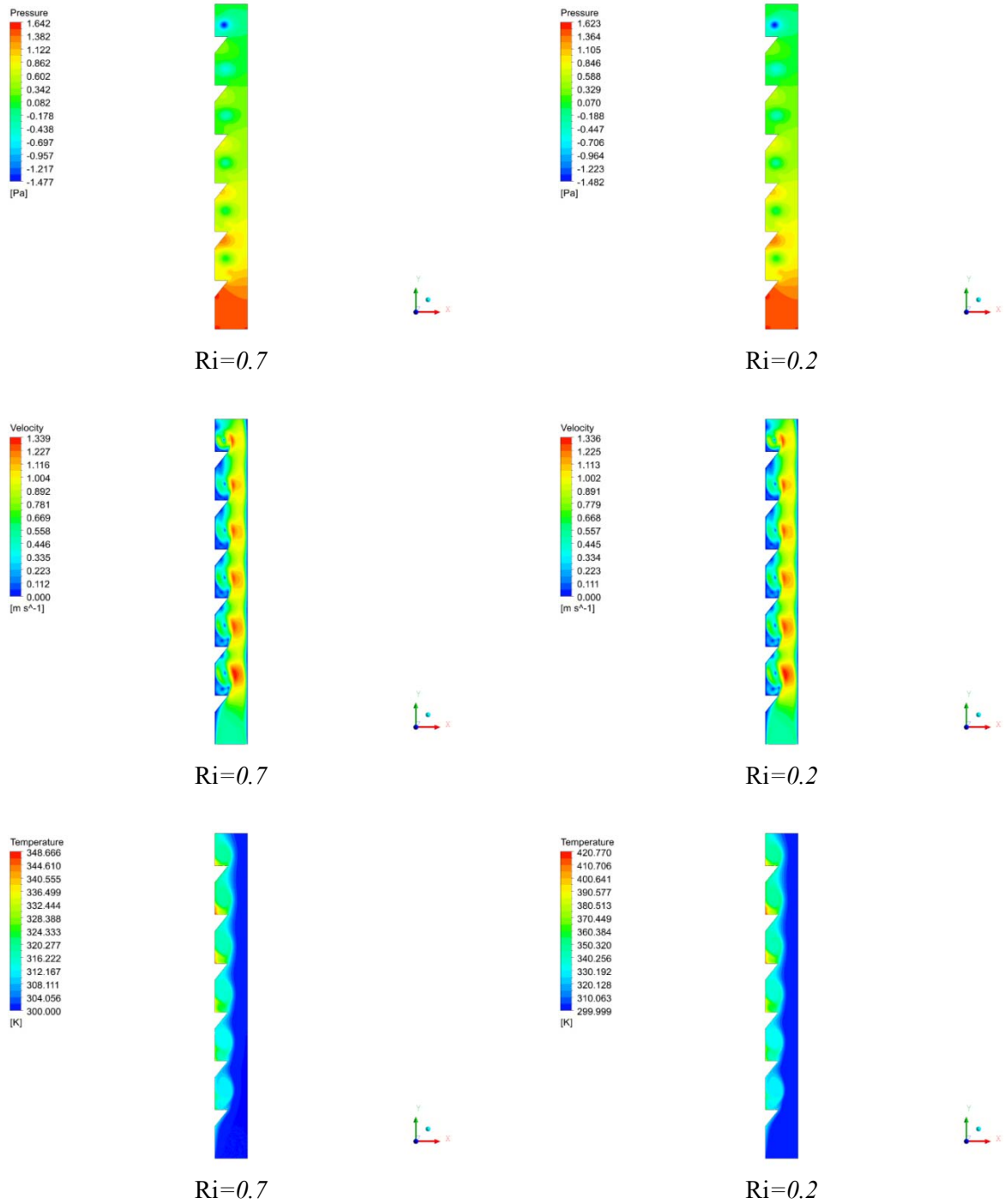

Fig.7. Pressure, velocity and temperatures countors of two parallel plates with triangular ribs upstream of air flow for ribs to height ratio of $w/W = 0.4$ and $\mathrm{Re} = 340$.

The distribution of relative temperatures in the cross sections of the channel at different triangular ribs heights is shown in Fig.5. One may note an improvement in the distribution of temperatures. Moreover, higher values of temperatures correspond to the higher level of heat transfer in case of using the ribs along the heated wall. From the analysis of Fig.5, it can be concluded that heat transfer reductions as the air moves along the height of the channel. Figure 6 presents the results of calculating the change in pressure, velocity and wall temperature along the height of the channel at various values of the Reynolds number. The distribution is periodic and the corresponding maximum and minimum exactly reflects the alternating nature of the location of the heated triangular ribs on the heated wall. The results showed that increasing the Reynolds number will lead to increasing the pressure drop and the velocity but at the same time it leads to decreasing the maximum temperatures inside the domain between the two parallel plates. Moreover, the effect of increasing the Richardson number on these air flow variables is presented in Fig.7. The results showed that decreasing the Richardson number has a counter effect on the pressure, velocity and temperature, thus the pressure and velocity will decrease but the temperature will increase due to increasing the effect of free convection.

The U-velocity profile between two parallel plates for different ribs to height ratio w/W values at $\mathrm{Re} = 340$ and $\mathrm{Ri} = 0.2$ is plotted in Figs 8-11 for upstream and downstream, respectively. The figure demonstrates the air velocity at the entrance at $y = 0.25$ and at the middle of the channel at $y = 0.5$. The maximum velocity at $\mathrm{Ri} = 0.2$ occurs near the cold wall when using the model of $w/W = 0.3$ and the maxumum velocity is found about $0.8\ m/sec$. The minimum velocity is observed when using the model of $w/W = 0.4$ for upstream ribs in the entrance region $y = 0.25$ as shown in Fig.8. Howevere, when the air flow reaches the middle region at $y = 0.5$, it shown in Fig.9 that the the maximum velocity is observed when using the model of $w/W = 0.4$ near the cold wall and the minimum velocity is found when using the model of $w/W = 0.0$. The curves have superior variations at $y = 0.5$ compared to $y = 0.25$ due to the air velocity at the top of the trangular rib. The results showed that increasing the Reynolds number will lead to high variations in velocity.

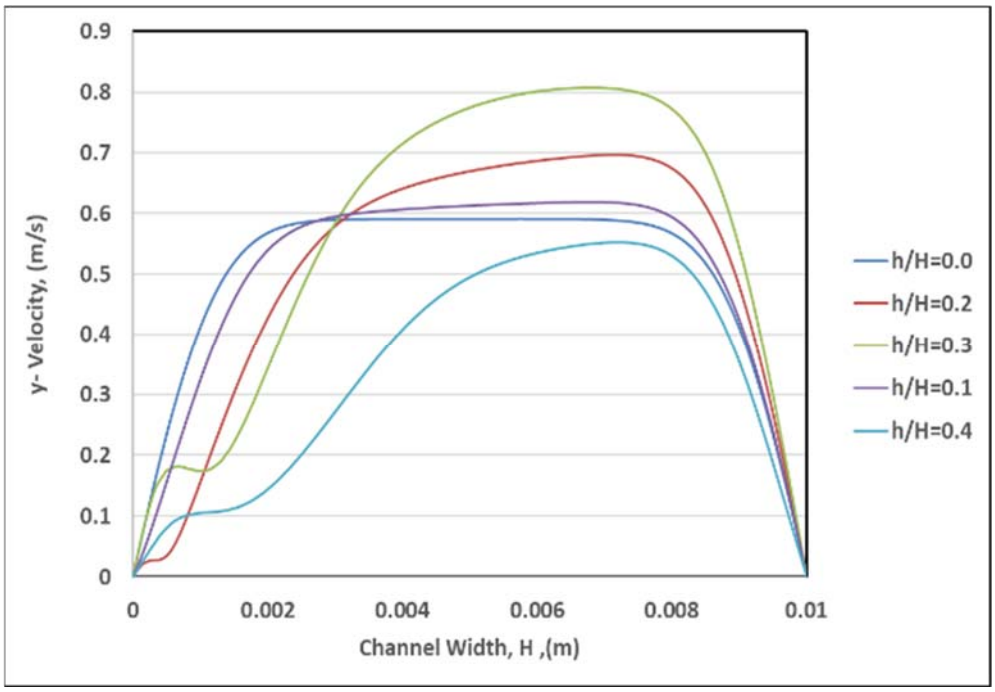

Fig.8. Velocity profile of air flow inside two parallel plates with upstream triangular ribs at entrance region $y/L = 0.25$ for various ribs to height ratio at $\mathrm{Re} = 340$ and $\mathrm{Ri} = 0.2$.

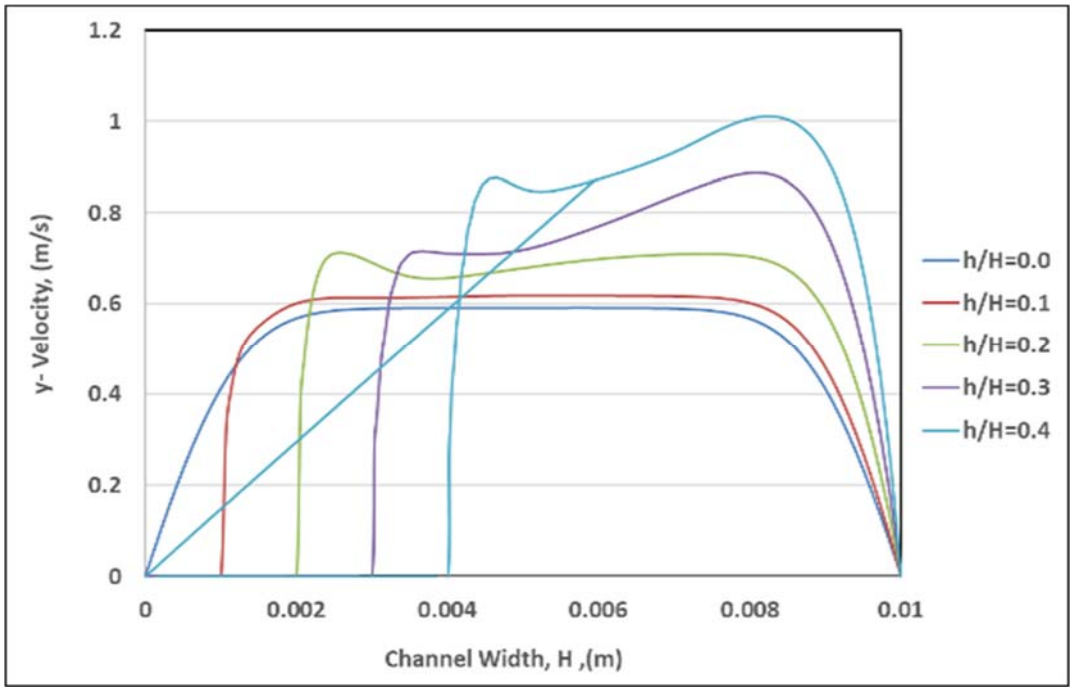

Fig.9. Velocity profile of air flow inside two parallel plates with upstream triangular ribs at entrance region $y / L = 0.5$ for various ribs to height ratio at $\mathrm{Re} = 340$ and $\mathrm{Ri} = 0.2$.

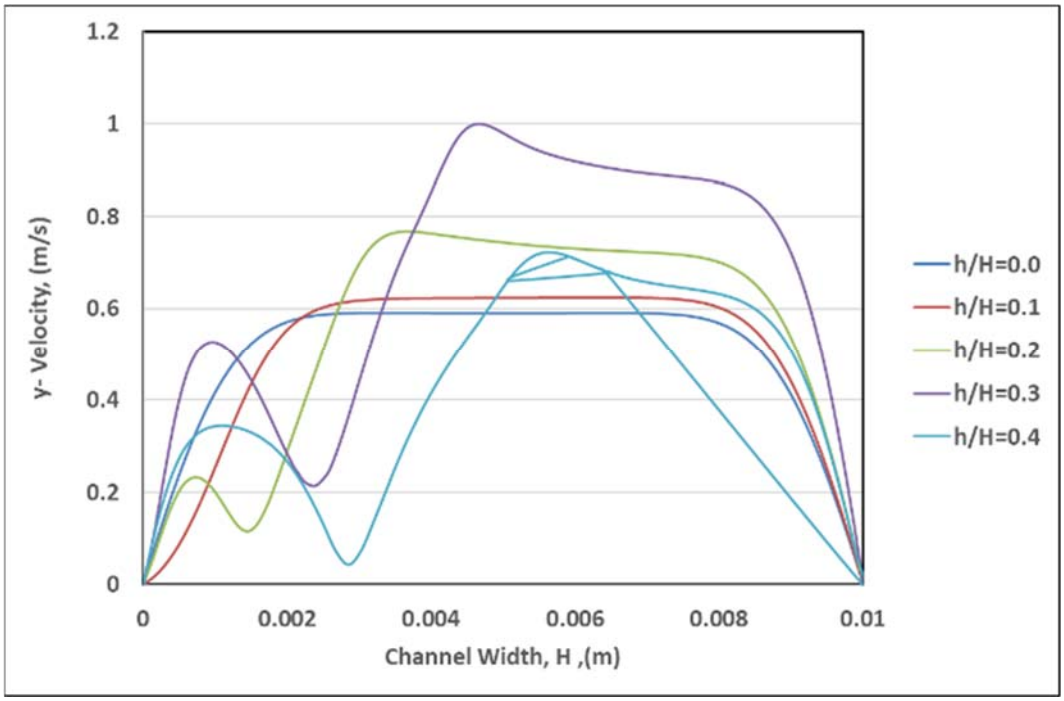

Fig.10. Velocity profile of air flow inside two parallel plates with downstream triangular ribs at entrance region $y / L = 0.25$ for various ribs to height ratio at $\mathrm{Re} = 340$ and $\mathrm{Ri} = 0.2$.

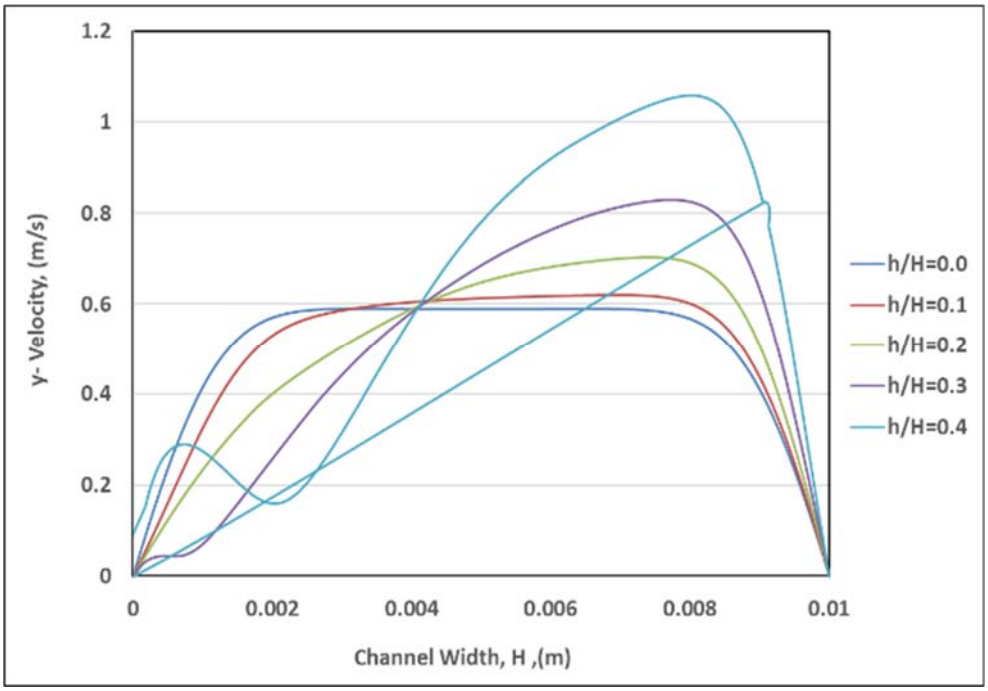

Fig.11. Velocity profile of air flow inside two parallel plates with downstream triangular ribs at entrance region $y / L = 0.5$ for various ribs to height ratio at $\mathrm{Re} = 340$ and $\mathrm{Ri} = 0.2$.

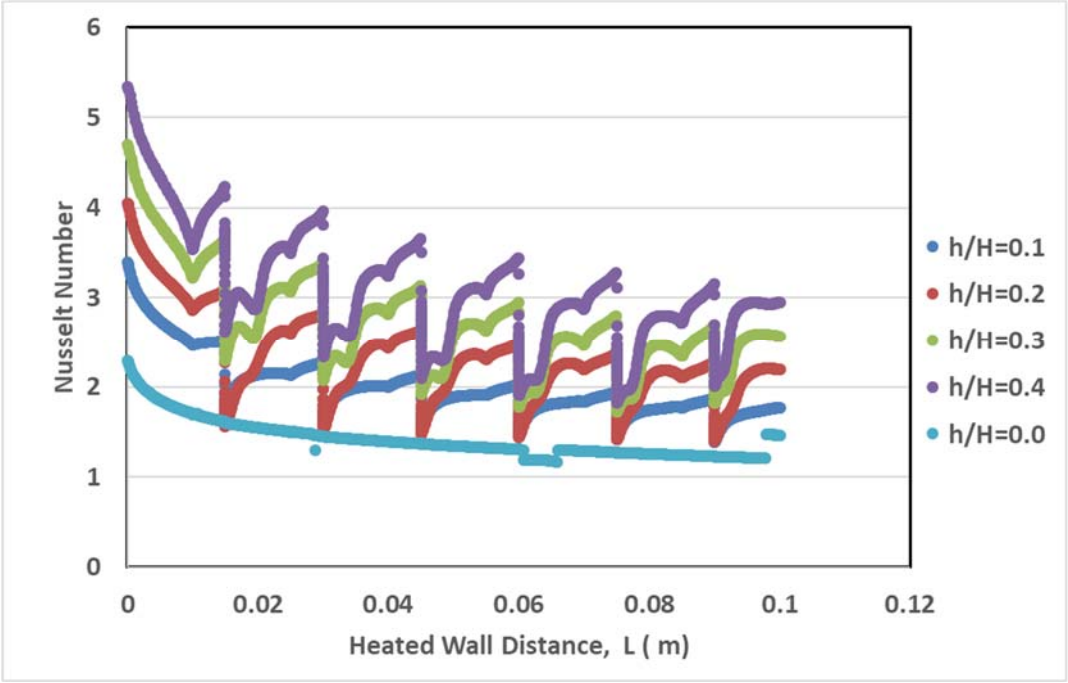

Fig.12. Variation of the Nusselt number with the length of the heated ribbed wall for air flow between two parallel plates with (upstream) triangular ribs at $\mathrm{Re} = 340$ and $\mathrm{Ri} = 0.2$.

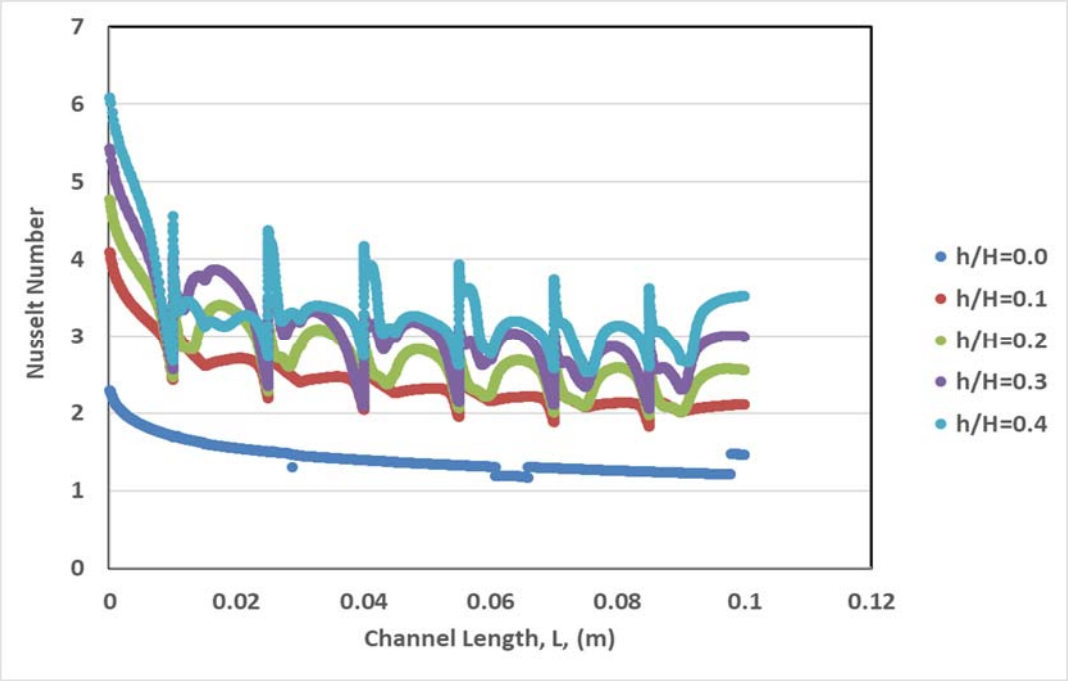

Fig.13. Variation of the Nusselt number with the length of the heated ribbed wall for air flow between two parallel plates with (dowstream) triangular ribs at $\mathrm{Re} = 340$ and $\mathrm{Ri} = 0.2$.

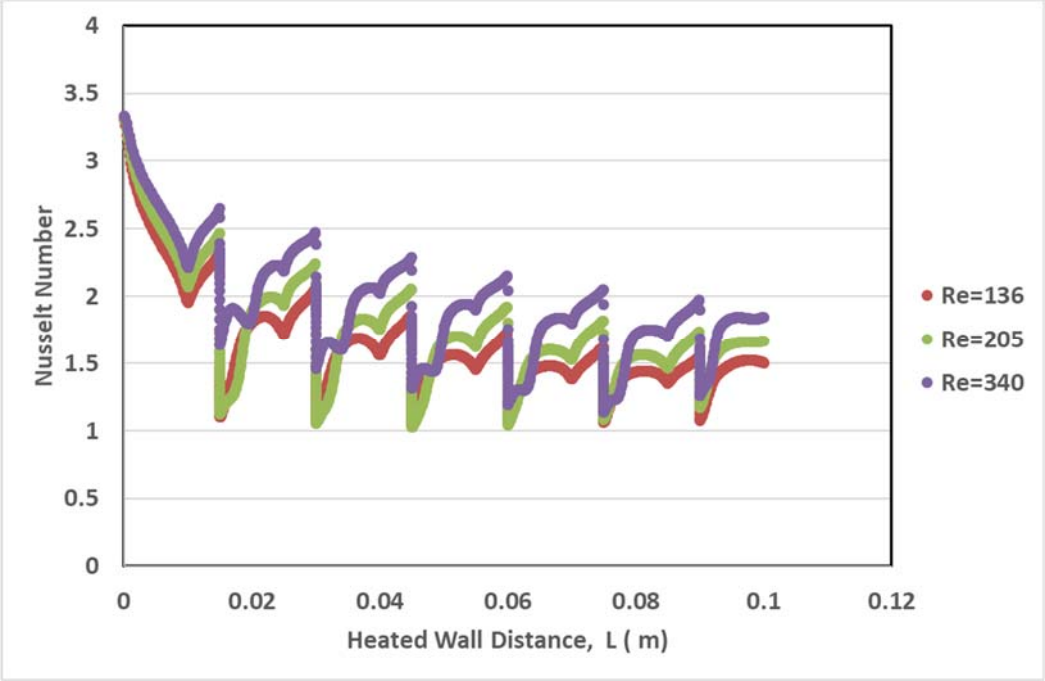

Fig.14. The local Nusslet number over the heated ribbed wall of the channel with variation of the Reynolds number and at constant Grashof number.

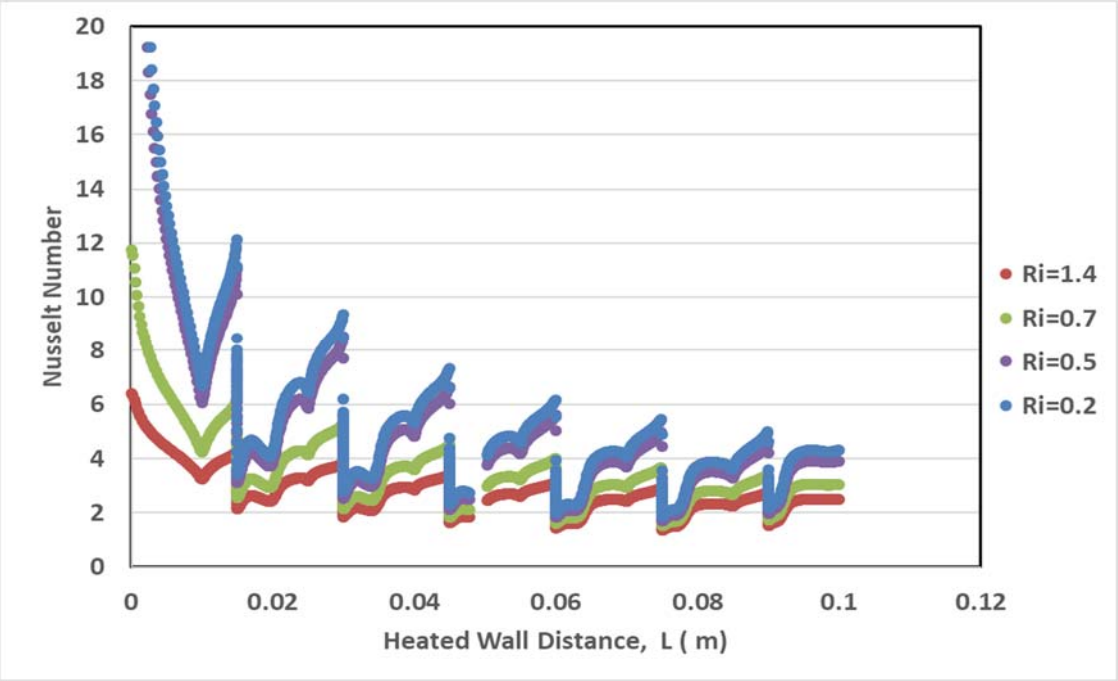

Fig.15. The local Nusslet number over the heated ribbed channel wall with variation of the Richardson number and at steady Grashof number.

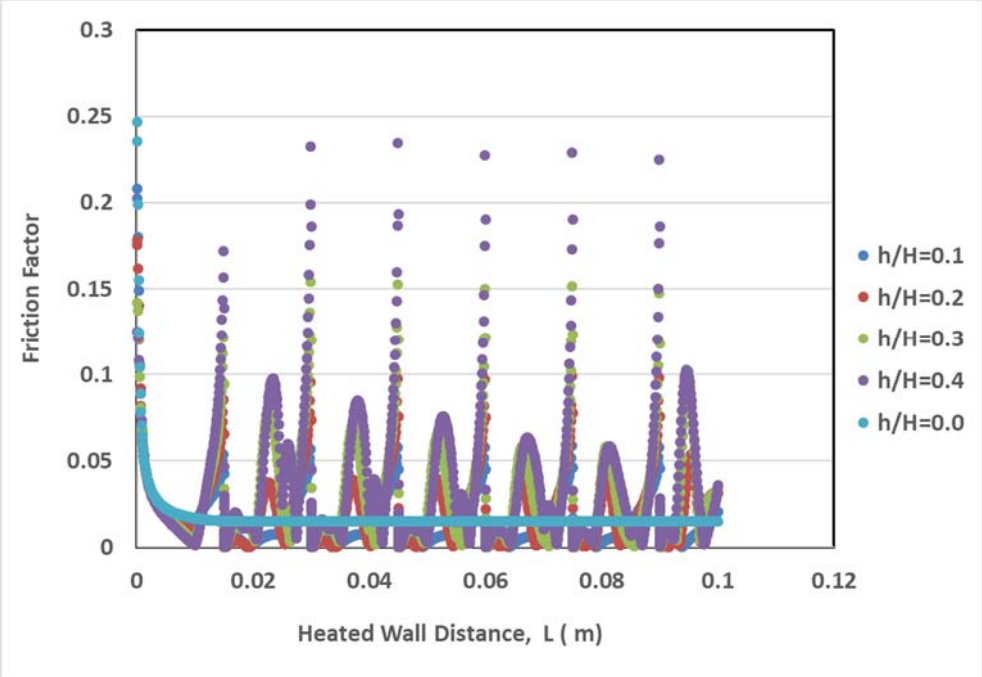

Fig.16. Variation of the friction factor with the length of the heated ribbed wall for air flow between two parallel plates with (upstream) triangular ribs at $\mathrm{Re} = 340$ and $\mathrm{Ri} = 0.2$.

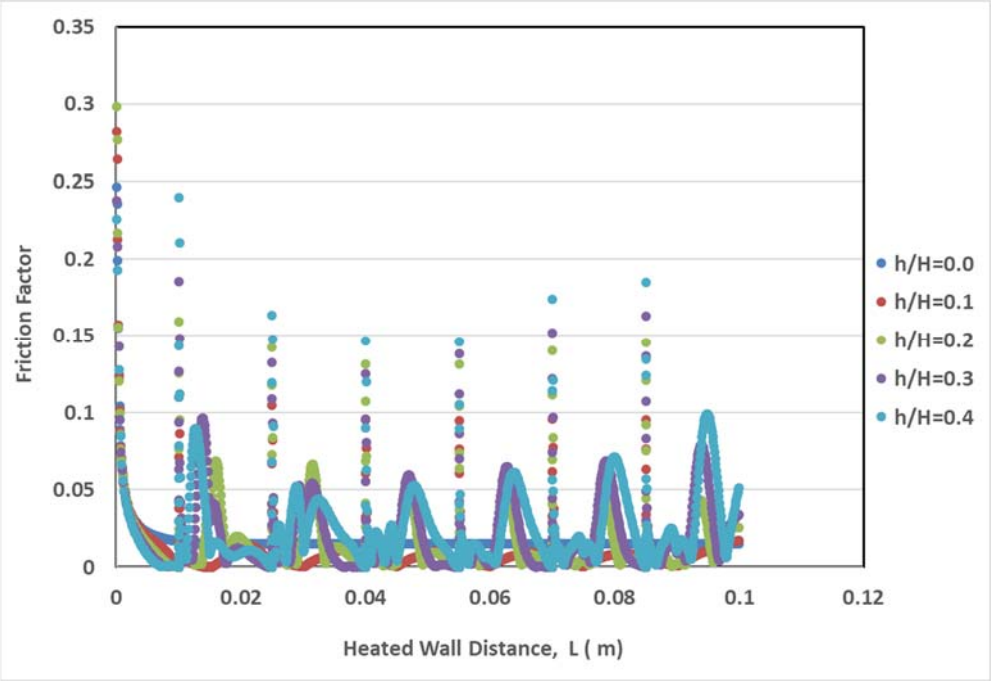

Fig.17. Variation of the friction factor with the length of the heated ribbed wall for air flow between two parallel plates with (downstream) triangular ribs at $\mathrm{Re} = 340$ and $\mathrm{Ri} = 0.2$.

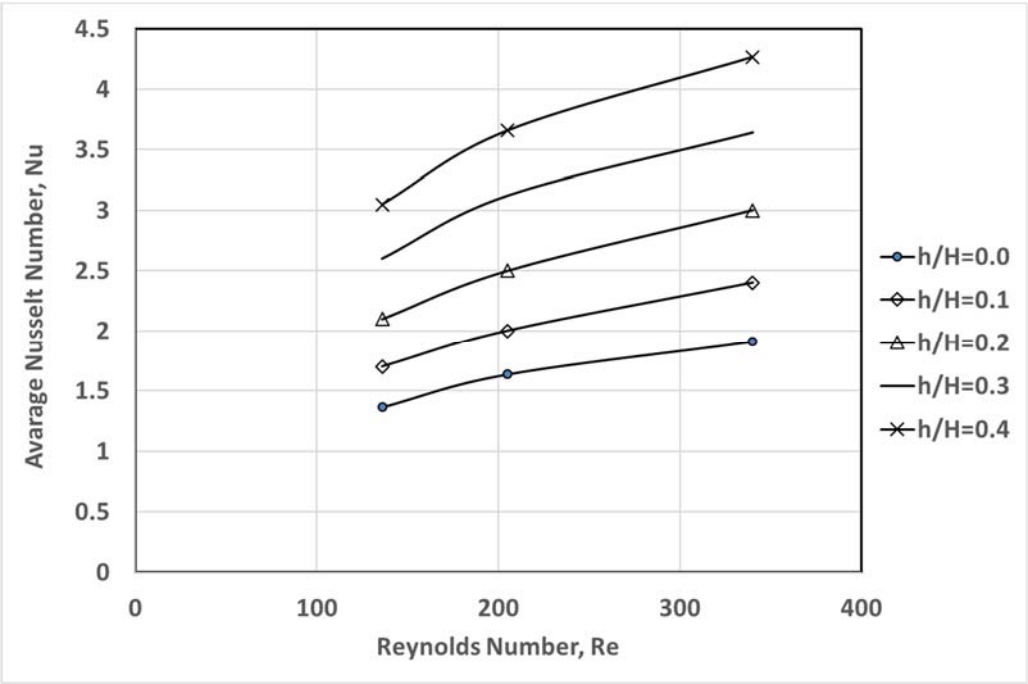

Fig.18. The average Nusslet number over the heated ribbed channel wall with variation of the Reynolds number and at steady Grashof number.

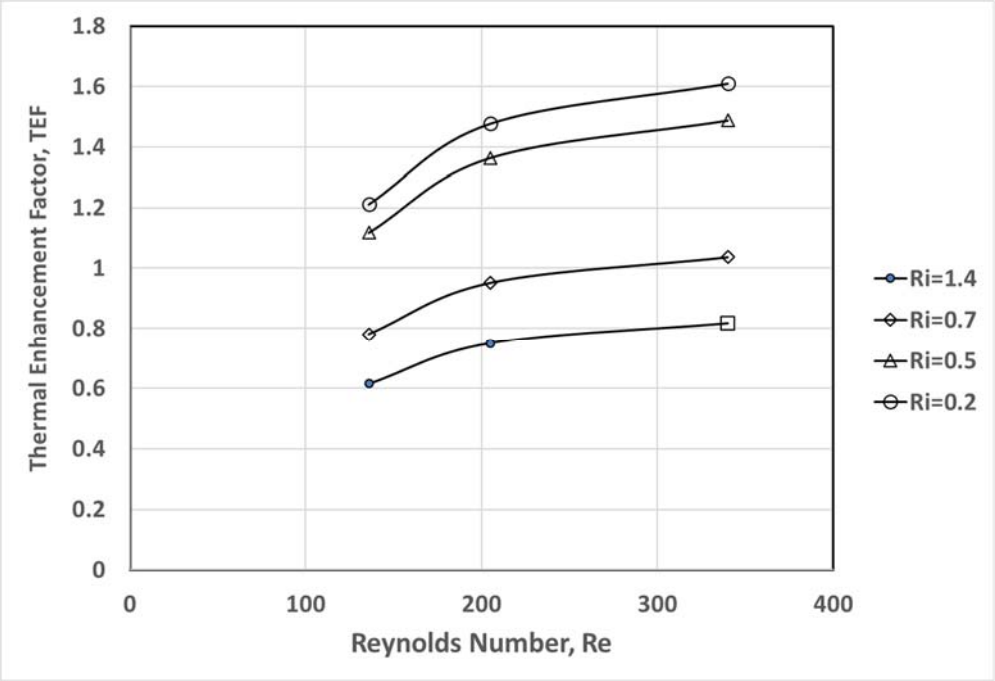

Fig.19. Variation of TEF with the Reynolds number.

The local values of the Nusselt number have a similar periodic and continuous distribution. These numerical data are presented for various upstream triangular ribs height and for downstream triangular ribs in Figs 12 and 13, respectively. The findings showed that the maximum value of the local heat transfer is achieved at the leading edge of each discrete element. Then it sharply decreases up to the trailing edge, where again the heat transfer coefficient slightly increases. A similar tendency is observed for all investigated regime parameters and variables. In both cases the Nusselt number is increased by increasing the ribs height ratio due to increasing the velocity near the heated wall. Also, the results showed that the maximum Nu increased by about 54% when using upstream ribs of $w/W=0.4$ compared with the smooth channel $w/W=0.0$ and by about 61% when using downstream ribs. This shows that using downstream ribs is the best choice for enhancing the heat transfer between the two parallel plates.

The behavior of the Nusselt numbers over each type of the ribs is shown in Fig.14 with changing the Reynolds number and with changing the Richardson number in Fig.15. The abscissa axis here indicates the numbers of triangular ribs. Depending on the location of the triangular ribs, the Nusselt numbers increased with increasing the Reynolds number and with decreasing the Richardson number. At the same time, there is a tendency to stabilize the thermal regime of the ribs that are far from the waste section. These features of the behavior of parameters in the discrete heating mode should be taken into account when analyzing systems with stepwise heat transfer. We proceed to the analysis of the results of the thermal averaged heat transfer over all discrete ribs.

Conclusions from the numerical results are plotted in Fig.15. In addition, under the considered conditions, there is no thermal stabilization mode when the Nusselt number is dependent upon the Reynolds number and Richardson number. This mode describes heat transfer in a stabilized section of the laminar flow between infinite parallel plates. In the region of low Reynolds numbers $\mathrm{Re}<200$, the average heat transfer is lower than during thermal stabilization, and for $\mathrm{Re}>200$ it becomes significantly higher. In the range $\mathrm{Ri}=0.1-1.4$, the contributions of both heat transfer mechanisms of forced and free convection are comparable, and the indicated boundaries coincide with the conclusions of the theory of mixed convection. Simultaneously, specificity of movement formation for discrete heating conditions affects the laws of heat transfer.

The effect of the height of heated ribs was studied for four values of $w/W = 0.0, 0.1, 0.2, 0.3$ and 0.4 at the same time, all other operating parameters remained constant. The results showed that the local heat transfer coefficients at the highest triangular ribs $h/H = 0.4$ were varied greatly along the surface of the ribs. Its maximum value is achieved at the interface between the front vertical and horizontal surfaces of the element. The forage face cools the worst, and here local overheating of the modules is possible. Moreover, the thermal picture stabilizes and becomes periodic already on the fourth to sixth elements. And, finally, it is obvious that the maximum heat transfer is observed on the first triangular rib, after it the heat transfer to the heated gas is several times lower.

In general, a similar picture is observed for other ratios of the h/H of the triangular ribs. Such a conclusion can be drawn from Figs 14 and 15, which show the development along the channel length of local heat transfer for all studied geometries of triangular ribs. For modules of various heights, the corresponding dimensions of the height and width of the triangular ribs were used as characteristic linear scales. The most intense heat transfer occurs on triangular ribs of $w/W = 0.4$. The heat transfer on the first triangular ribs is comparable with it. A noticeable decrease is observed with increasing triangular ribs height, which is mainly due to the influence of the formation of non-flowing vortex zones with a reduced level of heat transfer.

The dependence of the friction factor for the two cases of upstream and downstream triangular ribs is shown in Figs 16 and 17. The results showed that the total friction factor increases with increasing triangular ribs height ratio w/W for the two cases. But the downstream model gives the maximum values of the friction factor as compared with the smooth channel.

Despite the noted features of the influence of the height of the triangular ribs on the flow and heat transfer characteristics, it is necessary to mention the similarity of these processes. First of all, this concerns the regime with the prevalence of forced convection. However, the absolute friction factor values of the two-dimensional triangular ribs are higher than for a flat one. The change of the average Nu with the Re ranged between *136* and *340* is drawn in Fig.18 for state below examination. Also, the results show that rising the flow rate considerably increases the heat transfer due to the growth in velocity. The temperatures along the heated wall will drop significantly for high Reynolds numbers, Therefore, there is an opposite proportionality between increasing Re and temperatures of the heated wall. The maximum Nu is achieved for $\mathrm{Re} = 340$ while the lowest one is obtained for $\mathrm{Re} = 136$. The results showed that the average Nusselt number increased by *59%, 51%, 41%* and *25%* by using (*h/H=0.1, 0.2, 0.3* and *0.4*) respectively. Conclusively, Fig.19 plotted the variants of the thermal enhancement factor (TEF) with the flow Re for both cases of smooth and ribbed vertical channels. The TEF value enhances with the amplification of Re and thus, the Re provides greatest thermal improvement factor TEF. The highest TEF is about 1.612 at the uppermost Re.

5. Conclusion

A numerical study for mixed-convective heat transfer in the laminar mode showed a strong heterogeneity of the local Nusselt number and friction factor between two parallel walls with triangular ribs attached to the heated adiabatic wall. These numerical calculations are presented for several flow and heat transfer parameters such as the Reynolds number, Grashof number and Richardson number. The results show significant changes in the rates of heat transfer from individual heated triangular ribs depending their position and height and the angle of attack of the ribs (upstream and downstream). It is established that the average Nusselt number for the system of discrete triangular ribs between the two parallel plates over the channel height is not constant when the Reynolds number changes, as is the case in the classical laminar flow between parallel plates. The limits of the prevailing effect of mixed convection in total heat transfer are found. It is revealed that the boundaries of the change in convection regimes are determined by the geometry of the heated triangular ribs. The entire heat transfer from the complete system of elements weakly depends on the Grashof number, demonstrating the overwhelming contribution of forced convection in the conditions under consideration, and especially with increasing triangular ribs height. Finally, the results demonstrate that the local Nusselt number and friction factor increase with increasing the triangular ribs height ratio. The results

showed that the average Nusselt number increased by *59%, 51%, 41%* and *25%* by using (*h/H=0.1, 0.2, 0.3* and *0.4*) respectively.

Nomenclature

C_f – skin friction coefficient,

Cp – specific heat for air $\left[J \cdot kg^{-1} \cdot K^{-1}\right]$

f – friction factor

f_o – friction factor of smooth channel

Gr – Grashof number

H – channel height $[m]$

h – triangular ribs height $[m]$

L – channel height $[m]$

Nu – average Nusselt number

Nu_o – Nusselt number of smooth channel

$\mathrm{Nu}x$ – local Nusselt number

p – triangular ribs pitch $[m]$

k – thermal conductivity $[W / m \cdot K]$

P – pressure $[Pa]$

q – heat flux $\left[W / m^2\right]$

R – gas constant $[J / mol \cdot K]$

Re – Reynolds number

Ri – Richardson number

Pr – Prandtl number

T – temperature $[K]$

T_{in} – inlet temperatures in the x directions $[m / s]$

U, V – components of dimensionless velocity in the x, y directions

u – axial velocity $[m / s]$

u, v – components of velocity in the x, y directions $[m / s]$

u_{in} – velocity inlet in the x directions $[m / s]$

v – transverse velocity $[m / s]$

w – triangular ribs width $[m]$

X, Y – components of dimensionless Cartesian coordinates in the x, y directions

x, y – Cartesian coordinates

Δ – difference

θ – dimensionless temperature

μ – dynamic viscosity $[Pa\ s]$

v – kinematics viscosity $\left[m^2 / s\right]$

ρ – density $\left[kg / m^2\right]$

ϕ – variable to represent quantities of u, v and T

References

[1] Incropera F.P. (1988): *Convection heat transfer in electronic equipment cooling*.– J. Heat Transfer, vol.110, No.4b, pp.1097-1111.

[2] Chu R.C. (1986): *Heat transfer in electronic systems*.– Proceedings 8-th International Heat Transfer Conference, San Francisco, vol.1, pp.293-305.

[3] Tanda G., Fossa M., Leonardi E. and Menezo C. (2009): *Natural convection heat transfer from staggered discrete thermal sources*.– State-of-the-art, Int. Symp. on Convective Heat and Mass Transfer in Sustainable Energy, April 26 –May 1, Tunisia, pp.6-11.

[4] Madhusudhana R.G. and Narasimham G.S. (2007): *Laminar conjugate mixed convection in a vertical channel with heat generating components*.– Int. J. of Heat and Mass Transfer, vol.50, pp.3561-3574.

[5] Sawant S.M. and Gururaja R.C. (2008): *Conjugate mixed convection with surface radiation from a vertical electronic board with multiple discrete heat sources*.– Heat Mass Transfer, vol.44, pp.1485-1495.

[6] Kuznetsov G.V. and Sheremet M.A. (2006): *Modeling of thermos gravitational convection in a closed volume with local heat sources*.– Thermophysics and Aeromechanics, vol.13, No.4, pp.611-621.

[7] Sudhakar T., Shori A., Balaji C. and Venkateshan S. (2010): *Optimal heat distribution among discrete protruding heat sources in a vertical duct*.– ASME J. Heat Transfer, vol.132, No.1, p.9.

[8] Mallikarjun P. and Vaidya H. (2017): *Mixed convective fully developed flow in a vertical channel in the presence of thermal radiation and viscous dissipation*.– Int. J. of Applied Mechanics and Engineering, vol.22, No.1, pp.123-144.

[9] Basant K.J. and Michael O.O. (2018): *Mixed convection flow in a vertical channel with temperature dependent viscosity and flow reversal: An exact solution*.– International Journal of Heat and Technology, vol.36, No.2, June, pp.607-613.

[10] Saadi S., Benissaad S., Poncet S. and Kabar Y. (2018): *Effective cooling of photovoltaic solar cells by inserting triangular ribs: a numerical study*.– World Academy of Science, Engineering and Technology, International Journal of Energy and Environmental Engineering vol.12, No.7, pp.488-494.

[11] Samee M., Afzal A., Razak A. and Ramis M. (2019): *Temperature and location of hot spots variation with spacing in a vertical parallel plate channel: conjugate view*.– International Journal of Heat and Technology, vol.37, No.1, March, pp.153-160.

[12] Kahalerras H., Fersadoul B. and Nessab W. (2020): *Mixed convection heat transfer and entropy generation analysis of copper-water nanofluid in a vertical channel with non-uniform heating*.– SN Applied Sciences, vol.2, No.76, https://doi.org/10.1007/s42452-019-1869-2

[13] Abhijeet P.S. and Gururaja R.C. (2020): *Buoyancy-aided conjugate mixed convection with surface radiation from a vertical channel with multiple non-identical discrete heat sources*.– International Journal for Computational Methods in Engineering Science and Mechanics, DOI: 10.1080/15502287.2020.1718799.

Received: October 9, 2020

Revised: January 25, 2021